Electronic Supplementary Information

Air-stable and reusable nickel phosphide nanoparticle catalyst for the highly selective hydrogenation of D-glucose to D-sorbitol

Sho Yamaguchi,[a] Shu Fujita,[a] Kiyotaka Nakajima,[b] Seiji Yamazoe,[c] Jun Yamasaki,[d] Tomoo Mizugaki[a,e] and Takato Mitsudome*[a]

*E-mail: mitsudom@cheng.es.osaka-u.ac.jp

[a]Department of Materials Engineering Science, Graduate School of Engineering Science, Osaka University, 1-3 Machikaneyama, Toyonaka, Osaka 560-8531, Japan

[b]Institute for Catalysis, Hokkaido University, Kita 21 Nishi 10, Kita-ku, Sapporo 001-0021, Japan

[c]Department of Chemistry, Tokyo Metropolitan University, 1-1 Minami Osawa, Hachioji, Tokyo 192-0397, Japan

[d]Research Center for Ultra-High Voltage Electron Microscopy, Osaka University, 7-1, Mihogaoka, Ibaraki, Osaka 567-0047, Japan

[e]Innovative Catalysis Science Division, Institute for Open and Transdisciplinary Research Initiatives (ICS-OTRI), Osaka University, Suita, Osaka 565-0871, Japan

Table of Contents

1. Characterization of conventional Ni catalysts

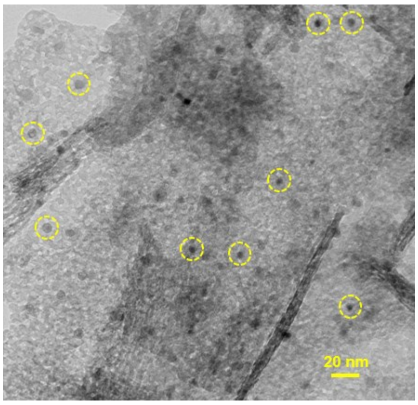

Fig. S1 Transmission electron microscopy (TEM) image of Ni/HT-Red.

The observation of Ni(II) in the XPS spectrum indicates that the supported Ni(0) nanoparticles must be oxidized, probably, during the XPS sampling (Fig. S2).

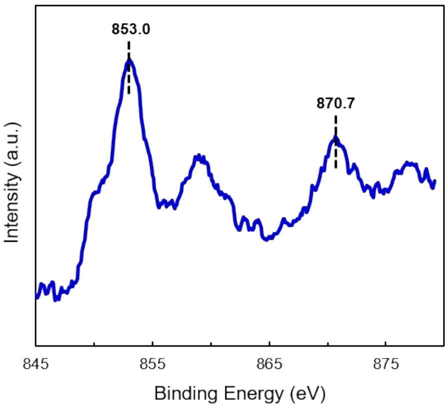

Fig. S2 X-ray photoelectron spectroscopy (XPS) spectra of Ni 2p of Ni/HT-Red.

2. Characterization of Ni phosphide catalysts

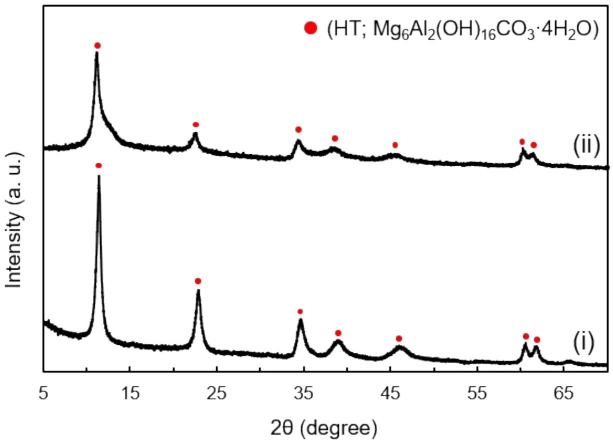

Fig. S3 X-ray diffraction (XRD) pattern of (i) hydrotalcite (HT) and (ii) fresh nano-Ni_2P/HT.

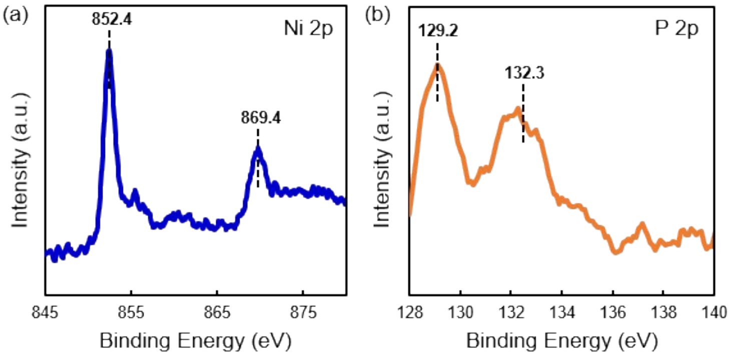

Fig. S4 XPS spectra of (a) Ni 2p and (b) P 2p of nano-Ni_2P/HT.

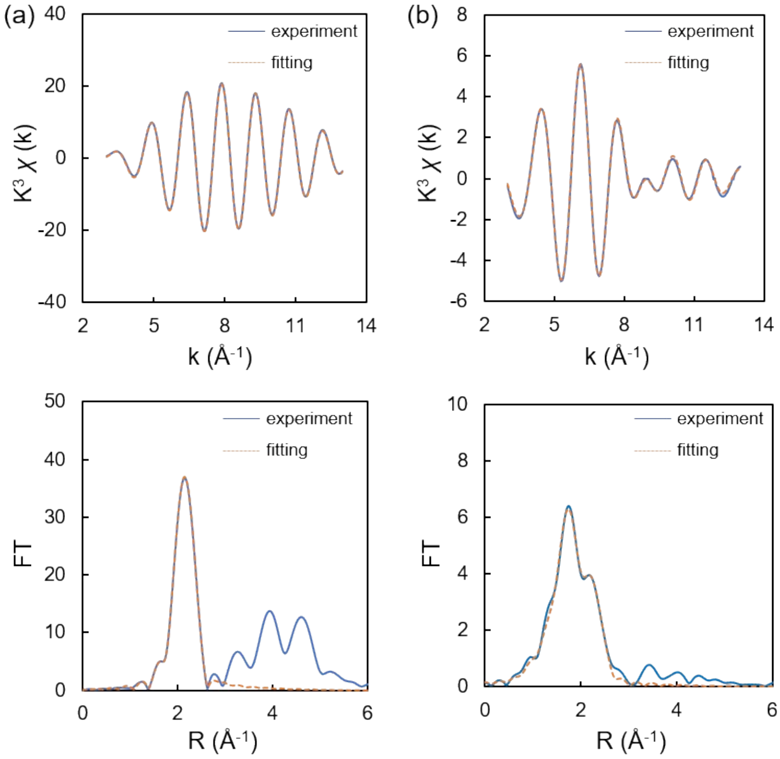

Fig. S5 Extended X-ray absorption fine structure (EXAFS) fitting curves in *k*-space (upper panel) and *R*-space (lower panel): (a) Ni foil and (b) nano-Ni_2P/HT.

Table S1 Curve fitting of Ni *K*-edge EXAFS spectra for Ni foil, nano-Ni_2P, and nano-Ni_2P/HT.

Sample	Shell	*CN* [a]	*R* (Å) [b]	DW [c]	R factor (%)
Ni foil	Ni–Ni	9.8 ± 0.1	2.48 ± 0.001	0.006 ± 0.00006	0.8
nano-Ni_2P/HT	Ni–P	3.0 ± 0.3	2.20 ± 0.002	0.009 ± 0.001	3.4
	Ni–Ni	2.7 ± 0.3	2.57 ± 0.002	0.012 ± 0.001	
bulk Ni_2P (ideal)	Ni–P[d]	2.2	2.24	——	——
	Ni–Ni[e]	6.7	2.65	——	

[a] Coordination number. [b] Bond distance. [c] Debye–Waller factor. [d] Average for Ni–P bonds with lengths less than 2.3 Å. [e] Average for Ni–Ni bonds with lengths less than 2.7 Å.

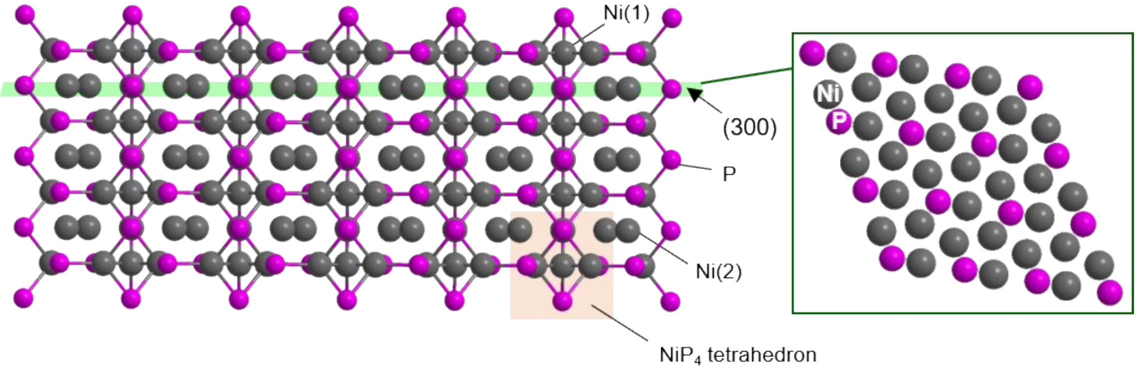

Fig. S6 Crystal structure of Ni_2P with a (300) plane.

3. Comparison of nano-Ni_2P/HT with previously reported catalysts

Table S2 Hydrogenation of D-glucose using various Ni or Co catalysts in batch systems.

Catalyst	Conditions	Yield of D-sorbitol [%]	TON	Ref.
nano-Ni_2P/HT	3 wt% D-glucose, 6.6 mol% Ni 100 °C, 20 bar, 2 h	99	15	***This work***
nano-Ni_2P/HT	3 wt% D-glucose, 13 mol% Ni 25 °C, 50 bar, 72 h	90	6.9	***This work***
nano-Ni_2P/HT	50 wt% D-glucose, 2.0 mol% Ni 100 °C, 50 bar, 18 h	92	46	***This work***
nano-Ni_2P/HT	20 wt% D-glucose, 0.10 mol% Ni 100 °C, 50 bar, 32 h	85	852	***This work***
Co-B amorphous alloy	50 wt% D-glucose, 12 mol% Co 120 °C, 40 bar, 6 h	89[a]	-	*S1*
Raney Ni-P	50 wt% D-glucose, 10 mol% Ni 120 °C, 40 bar, 6 h	56[a]	-	*S2*
Ni-B/SiO_2 amorphous alloy	50 wt% D-glucose, 3.7 mol% Ni 100 °C, 40 bar, 6 h	80[a]	-	*S3*
Commercial Ni/SiO_2	40 wt% D-glucose, 2.1 mol% Ni 120 °C, 120 bar, 5 h	35	16	*S4*
Ni/Al_2O_3	40 wt% D-glucose, 0.16 mol% Ni 120 °C, 120 bar, 5 h	28	172	*S4*
Commercial Ni/SiO_2	20 wt% D-glucose, 3.4 mol% Ni 120 °C, 120 bar, 5 h	60	18	*S5*
Ni/SiO_2	20 wt% D-glucose, 1.1 mol% Ni 120 °C, 120 bar, 5 h	42	39	*S5*
Ni powder	10 wt% D-glucose, 10 mol% Ni 120 °C, 30 bar, 2 h	7	0.23	*S6*
Ni-Al (alumel)	10 wt% D-glucose, 10 mol% Ni 120 °C, 30 bar, 2 h	4	0.28	*S6*

Ni-B amorphous alloy	20 wt% D-glucose, 22 mol% Ni 120 °C, 40 bar, 2 h	85[a]	-	*S7*
Ni/Cu/Al	4.7 wt% D-glucose, 15.5 mol% Ni 125 °C, 30 bar, 3 h	69	4.5	*S8*
Ni nanoparticles /AlOH	1.2 wt% D-glucose, 1.2 mol% Ni 130 °C, 20 bar, 24 h	93	81	*S9*
Ni-Co nanoalloy	25 wt% D-glucose, 11 mol% Ni, Co 90 °C, 30 bar, 4 h	97	8.5	*S10*
Ni/NiO	4.5 wt% D-glucose, 4.3 mol% Ni 150 °C, 50 bar, 4 h	88	20	*S11*
Ni-P amorphous alloy in the presence of Pd	10 wt% D-glucose, 27 mol% Ni 100 °C, 40 bar, 4 h	94[a]	-	*S12*

[a] Glucose conversion.

4. Gram-scale experiments

The nano-Ni_2P/HT catalyst (3.0 mol%) was applied to a gram-scale reaction using 3.0 g of D-glucose (40 mL distilled water, 40 bar H_2, 80 °C, 24 h). After the hydrogenation reaction, the autoclave was cooled in an ice-water bath and the H_2 gas was carefully released. The solid catalyst was removed from the reaction mixture by suction filtration and washed several times with water. The High-performance liquid chromatography refractive index detection (HPLC-RID) analysis of the filtrate showed the almost complete conversion of D-glucose to D-sorbitol (>99% yield), while a trace amount of D-mannitol was formed as a byproduct (Fig. S7). After evaporation of the filtrate to remove water, remaining trace water was removed as an azeotrope with toluene to give 3.0 g of pure D-sorbitol (>99% isolated yield).

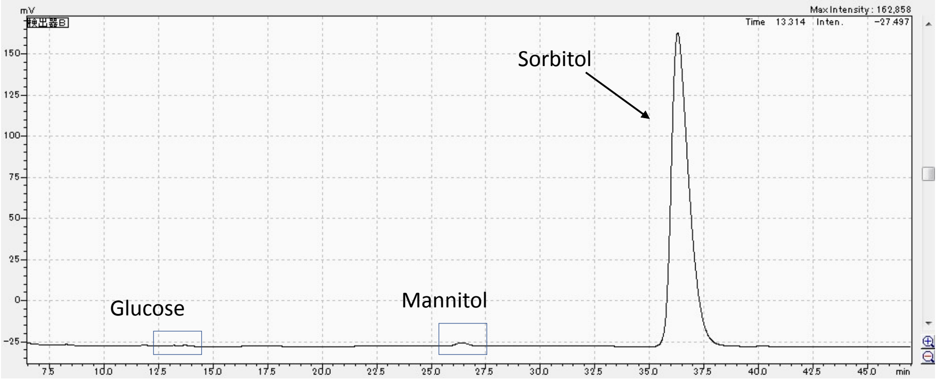

Fig. S7 High-performance liquid chromatography refractive index detection (HPLC-RID) chromatogram of the products from the gram-scale hydrogenation of D-glucose to D-sorbitol (Scheme 1a).

5. Recycling experiments

After the hydrogenation reaction was completed, the catalyst was separated from the reaction mixture by centrifugation, washed with deionized water, and reused in the next cycle without any pretreatment. This experiment was repeated four times.

6. Characterization of spent Ni phosphide catalysts

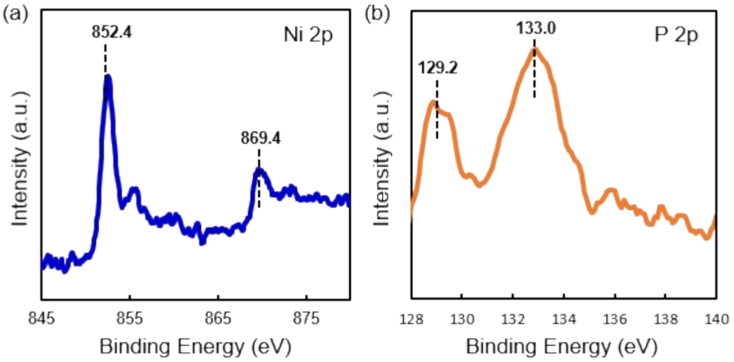

Fig. S8 XPS spectra of (a) Ni 2p and (b) P 2p of spent nano-Ni_2P/HT.

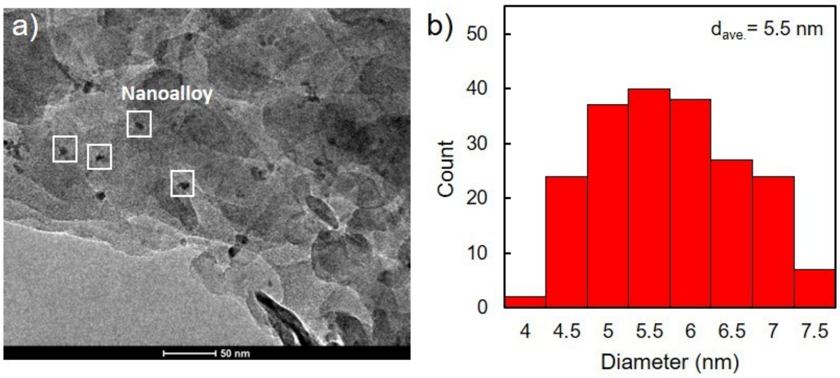

Fig. S9 (a) TEM image and (b) size distribution histogram of spent nano-Ni_2P/HT.

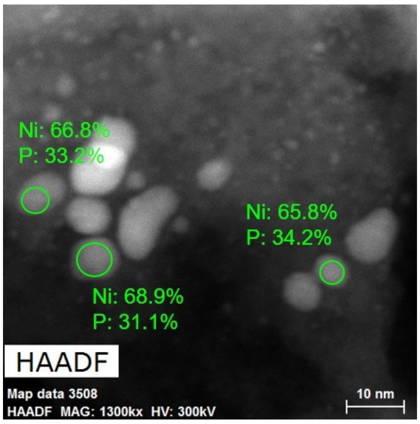

Fig. S10 Energy dispersive X-ray spectroscopy (EDX) analysis of spent nano-Ni_2P/HT in the regions indicated by green circles.

References

S1 (a) H. Li, H. Li, W. Wang and J.-F. Deng, *Chem. Lett.*, 1999, **28**, 629–630. (b) H. Li, H. Li and M. Wang, *Appl. Catal. A*, 2001, **207**, 129–137. (c) H. Li and J.-F. Deng, *J. Chem. Technol. Biotechnol.*, 2001, **76**, 985–990.

S2 H. Li, W. Wang and J. F. Deng, *J. Catal.*, 2000, **191**, 257–260.

S3 H. Li, H. Li and J.-F. Deng, *Catal. Today*, 2002, **74**, 53–63.

S4 B. Kusserow, S. Schimpf and P. Claus, *Adv. Synth. Catal.*, 2003, **345**, 289–299.

S5 S. Schimpf, C. Louis and P. Claus, *Appl. Catal. A*, 2007, **318**, 45–53.

S6 J. Zhang, L. Lin, J. Zhang and J. Shi, *Carbohydr. Res.*, 2011, **346**, 1327–1332.

S7 (a) J. Guo, Y. Hou, C. Yang, Y. Wang, H. He and W. Li, *Catal. Commun.*, 2011, **16**, 86–89. (b) J. Guo, Y. Hou, C. Yang, Y. Wang and L. Wang, *Mater. Lett.*, 2012, **67**, 151–153.

S8 J. Zhang, S. Wu, Y. Liu and B. Li, *Catal. Commun.*, 2013, **35**, 23–26.

S9 R. Rodiansono and S. Shimazu, *Bull. Chem. React. Eng. Catal.*, 2013, **8**, 40–46.

S10 Q. Dong, Y. Huang, H. Yang, J. Pei, K. Li, M. Yuan, W. Xiao, W. Ni and Z. Hou, *Top. Catal.*, 2017, **60**, 666–676.

S11 H. Singh, A. Rai, R. Yadav and A. K. Sinha, *Mol. Catal.*, 2018, **451**, 186–191.

S12 Y. Yang, H. Gu, Q. Zhang, H. Li and H. Li, *ACS Appl. Mater. Interfaces*, 2020, **12**, 26101–26112.